Quantitative analysis of carbon corrosion during fuel cell start-up and shut-down by anode purging

Nicolas Linse, Günther G. Scherer, Alexander Wokaun, Lorenz Gubler*

Electrochemistry Laboratory, Paul Scherrer Institut, OVGA/103, CH-5232 Villigen PSI, Switzerland

HIGHLIGHTS

► Carbon corrosion during PEFC start-up and shut-down by anode purging was investigated.
► Conclusions on effects related to the propagation of the gas front were drawn.
► In OCV mode, the gas exchange process is dominated by homogeneous gas displacement.
► The application of a load strongly influences shut-down induced corrosion behavior.

GRAPHICAL ABSTRACT
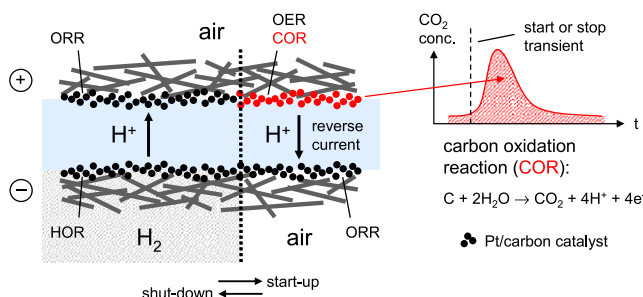
ARTICLE INFO

ABSTRACT

The corrosion of the carbon support during start-up and shut-down of polymer electrolyte fuel cells was systematically quantified to elucidate effects related to the propagation of the gas front through the anode compartment and to determine the influence of relevant operating parameters. Measurements with different reactant gas concentrations and gas flow rates suggest that the gas exchange process is dominated by a homogeneous displacement of the anode gas in case of start/stop operation at OCV. The influence of additional effects such as direct recombination of hydrogen and oxygen, diffusion on the channel and land scale and pseudocapacitive effects seems to be negligible under the investigated conditions. With an external load applied during the gas exchange process (discharge mode), shut-down induced carbon corrosion strongly differs from the behavior at OCV. The virtually constant corrosion rates obtained below a critical purge gas flow rate in the discharge mode are attributed to a significant contribution of electrochemical hydrogen consumption. Temperature and humidity variation measurements demonstrate that the carbon corrosion behavior during real start/stop processes can differ considerably from the correlations obtained under controlled potential conditions in H_2/N_2 mode. Thus, potential cycling experiments only provide limited information about start/stop durability under application relevant conditions.

1. Introduction

Carbon corrosion induced deterioration of the porous catalyst layer structure can strongly affect the performance of polymer electrolyte fuel cells (PEFCs). While carbon corrosion under ordinary PEFC operating conditions is usually considered to be negligible, the elevated potentials occurring at the positive electrode during fuel cell start-up and shut-down can strongly accelerate corrosion induced degradation. In the commonly used approach, the hydrogen present at the anode during ordinary PEFC operation is replaced by air to shut-down the fuel cell, and vice versa for start-up. During this process, a hydrogen/air front is formed, which propagates through the anode compartment of the

* Corresponding author. Tel.: +41 56 310 2673; fax: +41 56 310 4416.
 E-mail address: lorenz.gubler@psi.ch (L. Gubler).

cell. The resulting temporary coexistence of hydrogen and oxygen at the negative electrode divides the cell in two sections [1]. The section with hydrogen present at the negative electrode acts as a power source, which polarizes the electrodes in the air/air section, thereby driving the potential at the positive electrode to values significantly exceeding the effective oxygen potential of approximately 1 V. Besides the acceleration of the electrochemical dissolution of platinum, these elevated potentials can cause severe corrosion of the carbon nanoparticles acting as support material for the fuel cell catalyst (cf. Equation (1)). As a consequence, the highly porous catalyst layer structure can undergo substantial changes, which strongly affect the performance of the fuel cell [2,3].

$$C + 2H_2O \rightarrow CO_2 + 4H^+ + 4e^- \qquad (1)$$
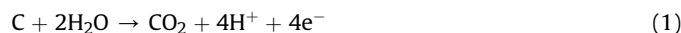
Due to the dynamic interaction of the hydrogen/air and the air/air section of the fuel cell, the potential conditions during the purging process are of high complexity. To allow a precise control of the corrosion−relevant parameters, the potentials developing at the positive electrode are therefore typically simulated by applying either a constant or cyclic external voltage to a cell operated in H_2/N_2 mode [4–17]. This simplified approach, however, which is essential to identify fundamental corrosion mechanisms, cannot provide information about effects related to the propagation of the hydrogen/air front through the anode compartment. Since the replacement of the anode gas is a crucial process determining the duration of the detrimental potential conditions, a comprehensive understanding of start/stop induced fuel cell degradation thus additionally requires a systematic analysis of parameters influencing the gas exchange process.

In several studies, the processes occurring during the propagation of the hydrogen/air front were investigated by measuring local current densities both along the direction of the flow field [18–21] and on the channel and land scale [22]. This approach offers the advantage of monitoring the gas exchange process with a good temporal and spatial resolution. A direct correlation between current density and carbon corrosion, however, is not possible. Besides the contribution originating from carbon corrosion, the total current density comprises charging of the electrochemical double layer, oxidation of the platinum catalyst particles and the oxygen evolution reaction. Since a precise discrimination between the different sources is not feasible, the determination of local current densities can thus only provide a rough estimate regarding the influence of different operating parameters on the carbon corrosion rate.

The commonly used method to directly quantify the amount of corroded carbon is to monitor the CO_2 concentration in the exhaust gas of the positive electrode (cf. Equation (1)). Although this method has been applied by several groups [4–9,12–14,23–29], no comprehensive study of parameters influencing the carbon corrosion behavior during fuel cell start-up and shut-down by purging of the anode compartment has been published so far.

In this study, the amount of evolved CO_2 was systematically quantified to elucidate effects related to the propagation of the gas front through the anode compartment and to analyze the influence of important operating parameters under real start/stop conditions. Although the integral determination of carbon corrosion rates cannot provide local information, measurements with different gas flow rates and reactant gas compositions allow conclusions about effects occurring along the direction of the flow field.

2. Experimental

All measurements in this study were performed using a single cell design with 16 cm² active area with parallel flow field (Fig. 1).
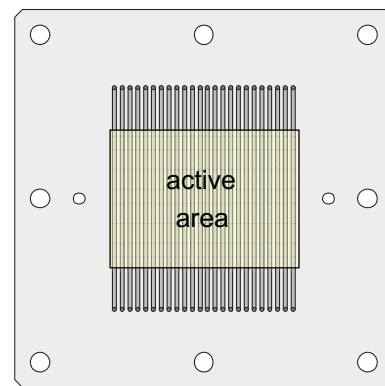

Fig. 1. Geometry of the single cell used in this study. The parallel flow field consists of 24 straight channels of 1 mm width and 1 mm depth, with a land width of 1 mm. The active area is 16 cm². Gas inlets are at the top, outlets at the bottom (co-flow mode).

The cell was operated in co-flow mode with gas inlets at the top. The volume of the flow channels in the active area is 0.816 mm³. This value is used later to estimate the residence time of the gas front in the cell. Gas diffusion electrodes, supplied by Johnson Matthey Fuel Cells (Swindon, UK), consist of a Toray TGP-H-060 carbon paper backing, which is coated with a microporous and catalyst layer (0.4 mgPt/cm², 60% Pt/C on high surface area carbon). The porosity of the Toray paper is 74−80% and the thickness of the electrode 192 ± 6 μm in uncompressed state. At a typical compression of 20% in the cell, the expected porosity is around 60%. MEAs were prepared by laminating Nafion® 212 (Fayetteville, USA), sub-gaskets (25 μm PEN from Goodfellow, Huntingdon, UK) and electrodes together and hot-pressing the assembly at a temperature of 120 °C using a compaction force of 8 kN for 3 min. The laminated MEA was assembled into the single cell fixture using PTFE gaskets of 0.1 mm thickness on both sides.

The cell was started up and operated for about 20 h at a temperature of 80 °C at a current density of 0.5 A cm^{-2} with fully humidified H_2 and O_2 at 2.5 bar$_a$ pressure. Direct water injection humidifiers (CEM, Bronkhorst, The Netherlands) were used for an accurate control of the humidity of the reactant gases. After around 20 h of conditioning, the cell was switched to OCV and H_2/N_2 operation mode at ambient pressure. After stabilization of the cell for around 1 h, 100 potential cycles between 0.6 V and 1.3 V (scan rate: 50 mV s^{-1}) were applied, using a Zahner IM6 or IM6e (Kronach, Germany) electrochemical workstation. Since the degradation behavior of pristine electrodes strongly changes during the repeated exposure to elevated potentials, this pre-degradation procedure is necessary to enable a reliable quantification of carbon corrosion rates. Subsequently, the effect of different parameters on start/stop induced corrosion of the catalyst support was determined by monitoring the CO_2 concentration in the exhaust gas of the positive electrode with a Model 100 Infrared Analyzer (California Analytical Instruments). To avoid flooding the CO_2 measurement cell, the water in the cathode exhaust was condensed by passing the effluent through a cold-trap containing a table salt saturated ice-water mixture. Start-up and shut-down of the fuel cell was performed by purging of the anode compartment with diluted or pure hydrogen and oxygen, respectively. The switching of the gas was performed up-stream to the humidifier using a 3/2-way solenoid valve (type 0330, Bürkert, Germany), which has a response time of 10−20 ms. All carbon corrosion rates were calculated by integration of the resulting CO_2 concentration peaks in the exhaust gas of the positive electrode. The carbon corrosion rate was calculated based on the ideal gas law and Faraday's law. For each investigated condition, the cell was exposed to eight start/stop transients. The time interval between the single

transients was 180 s in all cases. Since the corrosion rates slightly decrease after changing the investigated parameter, only the last three CO_2 concentration peaks were used to calculate the carbon corrosion rates.

To elucidate effects related to the propagation of the gas front through the anode compartment, corrosion rates were determined as a function of the gas flow rate at the negative electrode. Thereby, different compositions of hydrogen and oxygen in nitrogen were used as anode gas. To allow a reliable quantification of the CO_2 concentration in the exhaust gas, the positive electrode was continuously purged with synthetic air consisting of 21% O_2 in N_2 at a gas flow rate of 600 ml_n/min. All experiments with varied reactant gas concentrations were carried out without an external load (OCV mode) at a temperature of 50 °C and a relative humidty of the reactant gases of 70% to avoid flooding of the electrodes. The reduced temperature of 50 °C was necessary because at the standard operating temperature of 80 °C the rate of carbon corrosion is so substantial that the positive electrode undergoes excessive degradation during the test. The influence of an applied external resistance on the carbon corrosion behavior could be investigated at 80 °C using pure hydrogen and air as reactant gases: due to the reduced potential developing at the positive electrode as a result of the application of an external load, the driving force for carbon corrosion is significantly reduced.

The effect of temperature and relative reactant gas humidity was determined at a constant gas flow rate of 600 ml_n min^{-1}. Both measurements were carried out with pure hydrogen and air while an external load of 3 Ωcm^2 was applied to the cell. Humidity variation experiments were performed at 80 °C. To avoid electrode flooding, the influence of temperature was investigated at a relative humidity of 70%.

3. Results and discussion

3.1. Effect of gas front propagation

Since the duration of the detrimental potential conditions is determined by the coexistence of hydrogen and oxygen at the negative electrode, CO_2 evolution rates during start-up and shut-down of the fuel cell strongly depend on the time that is necessary for a complete exchange of the anode gas. Accordingly, an increase in the gas flow rate at the negative electrode generally leads to a decrease of the carbon corrosion rates (cf. Fig. 2). Furthermore, the absolute amount of evolved CO_2 obtained for start-up and shut-down processes strongly depend on the composition of the reactant gases. Fig. 2 shows that the concentration of hydrogen influences carbon corrosion mainly during shut-down of the fuel cell. Depending on the gas flow rate, a change in hydrogen content from 5% to 100% increases the carbon corrosion rates by more than a factor of 20. In case of fuel cell start-up, however, the effect of hydrogen concentration is less pronounced. While an increase from 5% to 21% does not significantly influence the carbon corrosion rates, the use of pure hydrogen decreases the CO_2 evolution rates by a factor of up to three. At low gas flow rates, however, the corrosion rates approach the values obtained in measurements carried out with diluted hydrogen.

This strong effect of hydrogen concentration on the carbon corrosion behavior can be based on several processes. Generally, the amount of evolved CO_2 is determined by the potential developing at the positive electrode during start-up and shut-down and the time for which the electrode is exposed to the elevated potentials. Both parameters can be influenced by the hydrogen content. According to the Nernst equation, an increase in hydrogen concentration from 5% to 100% decreases the potential at the negative electrode in the normal operation section of the fuel cell
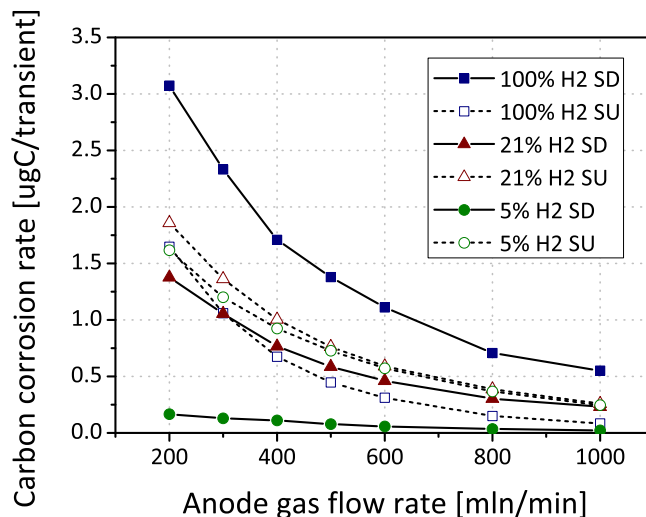

Fig. 2. Carbon corrosion rates determined for start-up (SU) and shut-down (SD) processes as a function of the anode gas flow rate for measurements carried out with different hydrogen concentrations. The oxygen concentration was 21% in all cases.

by about 46 mV. This leads to a higher driving force for carbon corrosion in the air/air section of the cell. This effect is expected to be independent of the gas flow rate at the anode. In addition, the effect of hydrogen concentration is likely to be influenced by processes affecting the duration of the gas exchange process. The amount of CO_2 evolved during start-up and shut-down of the fuel cell can thus be assumed to be mainly determined by the time that is necessary to completely remove hydrogen or oxygen from the anode compartment. Since this process would be largely independent of the reactant gas composition in case of pure plug flow, the observed effect of hydrogen concentration suggests that the exchange of the anode gas is strongly affected by diffusion processes in the GDL and the catalyst layer of the negative electrode. This strong influence of diffusion phenomena is supported by the fact that the effective duration of the gas replacement process was found to be significantly higher than the calculated residence time of the gas front [30].

Despite this difference, the correlation between the theoretical duration of the gas replacement process and the corresponding CO_2 evolution rates can provide valuable information about the mechanisms controlling the exchange of the anode gas. In Fig. 3, carbon corrosion rates are plotted as a function of the theoretical gas front residence time, which was calculated by dividing the total volume of the channels in the anode flow field (816 mm^3) by the respective flow rates, taking into consideration the temperature and partial pressure of the gas. Under all investigated conditions, corrosion rates for both start-up and shut-down processes show an essentially linear increase with increasing gas front residence time. Only in case of the lowest investigated gas flow rate of 200 ml_n min^{-1}, the corrosion rates slightly deviate from the linear trend. This indicates that the contribution of processes influencing the amount of evolved CO_2 does not markedly change in the investigated gas flow range. In their pseudo-capacitive model, Gu et al. suggested that the generation of local currents originating from platinum oxidation/reduction and the adsorption/desorption of hydrogen can strongly decrease carbon corrosion rates during fuel cell start-up and shut-down [31]. Due to the short duration of these pseudo-capacitive currents, the influence of this effect was proposed to strongly depend on the gas flow rate at the negative electrode. Generally, short gas front residence times are assumed to cause the most pronounced decrease in carbon corrosion rates. Yet, although
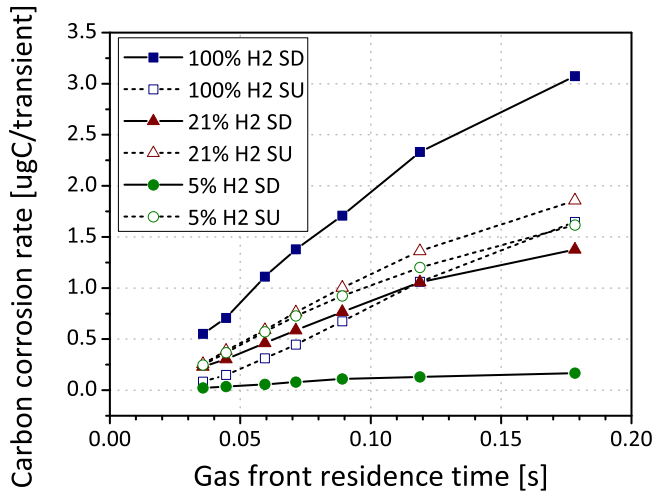
Fig. 3. Carbon corrosion rates determined for start-up (SU) and shut-down (SD) transients as a function of the theoretical gas front residence time for measurements carried out with different hydrogen concentrations. The residence time was calculated by dividing the total volume of the channels in the anode flow field by the respective gas flow rates.

the investigated front durations are in the order in which the pseudo-capacitive effect is expected to significantly influence CO_2 evolution behavior, the corrosion rates show a roughly linear increase with increasing gas front residence time. This linear correlation strongly indicates that the mitigating effect of pseudo-capacitive currents does not change in the investigated gas flow range. This behavior might partly be explained by the discrepancy between the theoretical gas front residence time and the effective duration of the gas exchange process. Ishigami et al. have shown that the two values can differ by a factor of seven [30]. However, even if this difference is considered, the pseudo-capacitive effect would be expected to cause marked deviations from the linear correlation between carbon corrosion rate and front residence time. Hence, under the investigated conditions, the influence of capacitive currents seems to be considerably lower than predicted by the model proposed by Gu et al.

Furthermore, the linear correlation demonstrates that the replacement of the anode gas during start-up and shut-down of the fuel cell is primarily controlled by processes occurring along the direction of the flow field. Extrapolation of the carbon corrosion rates to a gas front residence time of zero seconds yields values around zero µgC/transient, indicating that contributions from additional processes with shorter time constants can be largely neglected. This is in stark contrast to results reported by Schneider and von Dahlen, who found that diffusion of the purging gas under the lands of the flow field can significantly influence the gas exchange process [22]. By means of submillimeter resolved current density measurements, they showed that these diffusion processes can induce reverse current phenomena also on the channel and land scale. Yet, the duration of the gas exchange processes in these experiments was always below 25 ms. In case of these low gas front residence times, channel and land effects might become significant since the contribution of corrosion processes caused by the front propagation through the flow field channels substantially decreases. Under the conditions investigated in the present study, however, start/stop induced carbon corrosion behavior is obviously not markedly influenced by gas diffusion under the flow field lands. This is supported by the fact that gas flow variation measurements with different channel and land dimensions of 1, 2 and 4 mm yielded very similar carbon corrosion rates (data not shown).

The constant ratios between carbon corrosion rates determined for shut-down and start-up transients in case of measurements carried out with diluted hydrogen furthermore indicate that the electrochemical consumption of hydrogen during the purging process does not markedly influence the replacement of the anode gas. Accordingly, the gas exchange process can be assumed to be dominated by a uniform displacement of the anode gas along the direction of the flow field.

The different effect of hydrogen concentration on start-up and shut-down induced catalyst support corrosion can thereby be explained by processes determining the duration and the impact of the detrimental potential conditions. Due to the substantially higher exchange current density, the electrode potential is generally dominated by the presence of hydrogen. Accordingly, small amounts of hydrogen at the negative electrode can cause carbon corrosion in large areas of the positive electrode. In case of fuel cell shut-down by purging of the anode compartment with air, the duration of the detrimental potential conditions is therefore determined by the time required to completely remove hydrogen from the negative electrode. Due to the high diffusivity of hydrogen and the fact that the gas front does obviously not propagate via ideal plug flow, the duration of this process significantly depends on the initial amount of hydrogen in the anode compartment. As a consequence, shut-down induced carbon corrosion strongly increases with increasing hydrogen concentration.

Correspondingly, start-up of the fuel cell requires the removal of air from the negative electrode. Thereby, if the anode compartment is purged with diluted hydrogen, the oxygen is mainly replaced by nitrogen. The similar carbon corrosion rates obtained in this case indicate that the duration of the gas exchange is mainly controlled by the flow rate and not by processes depending on the composition of the purging gas. In contrast, start-up of the fuel cell with pure hydrogen leads to considerably lower carbon corrosion rates. This effect might be based on the substantial change in the diffusion coefficient, which increases by a factor of almost four compared to the replacement of the oxygen at the anode by mainly nitrogen [32]. Due to the fact that the local potential at the negative electrode is dominated by the presence of hydrogen, a fast propagation of hydrogen into the air-filled areas can significantly decrease the duration of the detrimental potential conditions [25]. Thereby, since catalyst support corrosion is limited to areas with oxygen present at the negative electrode, the effect of flow rate can be assumed to be more pronounced than in case of fuel cell shut-down, thus leading to the varying ratio of the carbon corrosion rates obtained for the two processes.

The effect of oxygen concentration on start/stop induced carbon corrosion behavior is shown in Fig. 4. For both start-up and shut-down processes, CO_2 evolution rates significantly increase with increasing oxygen content. Thereby, analogous to the investigations on the effect of hydrogen concentration, all measurements yielded a linear correlation between carbon corrosion rates and calculated duration of the gas exchange process. Extrapolation to infinitely low front residence times results in slightly negative carbon corrosion rates. Yet, in contrast to measurements with different hydrogen concentrations, the ratio between carbon corrosion rates determined in response to start-up and shut-down transients was found to be independent of both gas flow rate and oxygen concentration. This constant ratio further indicates that the replacement of the anode gas is not markedly influenced by the electrochemical consumption of the reactant gases. As discussed for varied hydrogen concentrations, a significant contribution of this effect would be expected to result in a considerable influence of gas front residence time and oxygen content on the start/stop ratio.

Moreover, the observed corrosion behavior shows that also the direct recombination of hydrogen and oxygen at the platinum
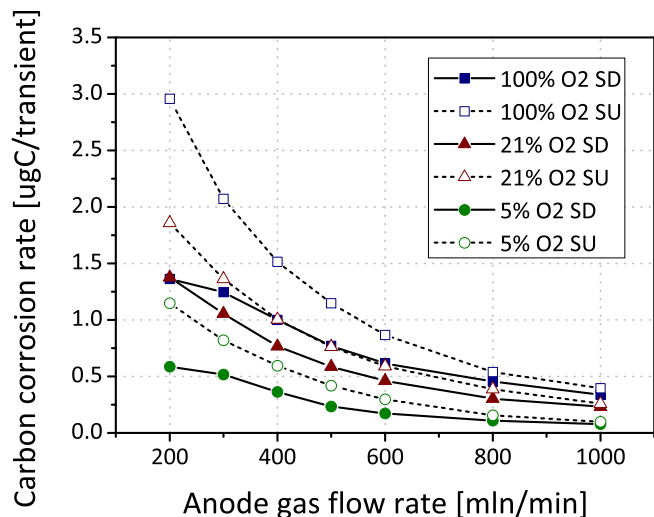
Fig. 4. Carbon corrosion rates determined for start-up (SU) and shut-down (SD) processes as a function of the anode gas flow rate for measurements carried out with different oxygen concentrations. The hydrogen concentration was 21% in all cases.

catalyst particles is negligible with respect to the duration of the gas exchange process. Due to the fact that the formation of water requires hydrogen and oxygen in the ratio 2:1, the catalytic reaction of those gases in the anode compartment accelerates the shut-down process while the duration of fuel cell start-up is increased. The recombination rate can thereby be assumed to generally increase with increasing reactant gas concentration. Thus, if a significant amount of hydrogen and oxygen would react with each other during the purging process, variations in the reactant gas composition would cause changes in the ratio between start-up and shut-down induced carbon corrosion.

Although all mentioned processes might slightly influence fuel cell start-up and shut-down, the corrosion behavior obtained for different flow rates and reactant gas compositions strongly indicates that the exchange of the anode gas is controlled by a simple displacement mechanism. Thereby, due to the high diffusivity and the dominating effect on the electrode potential, the duration of the detrimental potential conditions seems to be mainly determined by the hydrogen concentration. However, although the results suggest that the oxygen content does not significantly affect the duration of the gas exchange process, an increase in the concentration strongly increases the carbon corrosion rates. This considerable effect of oxygen content might be based on two processes influencing the detrimental potentials leading to carbon corrosion at the positive electrode. First, a decrease in oxygen concentration results in a lower equilibrium potential at the negative electrode in the air/air section of the fuel cell. Compared to the pure gas, a decrease in oxygen content to 5% reduces the equilibrium potential by about 21 mV. Since this potential drop causes a similar decrease in the potential of the positive electrode, the amount of oxygen in the reactant gas directly influences the driving force for carbon corrosion. Second, the oxygen content influences the polarization behavior of the negative electrode, thus leading to a further potential decrease in case of measurements carried out with diluted oxygen. Yet, since the total current in the air/air section originates from several interacting processes, the effect of oxygen content on the electrode polarization cannot be assessed quantitatively. Due to the exponential correlation between electrode potential and carbon corrosion rate, however, a comparatively low potential drop can already cause a significant reduction in CO_2 evolution. Measurements under controlled potential conditions

have shown that a decrease in the electrode potential by 50 mV can decrease the corrosion rates by more than a factor of two [33]. Thus, assuming that a lower oxygen concentration markedly influences the polarization behavior of the negative electrode, the resulting overall potential drop at the positive electrode can explain the observed decrease in CO_2 evolution.

3.2. Effect of the external resistance

All measurements described in Section 3.1 were carried out under OCV conditions to keep the processes occurring during the exchange of the anode gas as simple as possible. Yet, owing to the decrease in the detrimental potentials developing at the positive electrode, start-up and shut-down is usually performed while an external load is connected to the cell. This is referred to as "discharge mode" since residual hydrogen or oxygen is electrochemically consumed. To analyze the resulting changes in the carbon corrosion behavior, gas flow variation experiments with an external resistance of 3 Ωcm^2 connected to the cell were carried out. Since the application of the load strongly decreases the driving force for carbon corrosion at the positive electrode, CO_2 evolution rates are substantially lower than in case of measurements carried out in OCV mode. To obtain CO_2 concentration peaks that allow a reliable quantification of start/stop induced carbon corrosion, the temperature was therefore increased to 80 °C. All measurements were carried out with air at the positive and the negative electrode.

Fig. 5 shows that the effect of the applied resistance strongly differs for start-up and shut-down transients. In case of fuel cell start-up, the correlation between anode gas flow rate and CO_2 evolution is similar to that obtained under OCV conditions. This indicates that the applied load primarily influences the detrimental potentials developing at the positive electrode. The gas exchange process at the negative electrode does not seem to be markedly affected. In contrast, shut-down induced carbon corrosion behavior strongly changes if an external resistance is connected to the cell. For measurements with pure hydrogen and gas flow rates up to 400 ml_n min^{-1}, CO_2 evolution basically follows the linear correlation between corrosion rates and calculated gas front residence time that was also obtained under OCV conditions. Yet, a further decrease in the flow rate to values smaller than 400 ml_n min^{-1} leads to an abrupt change in the carbon corrosion behavior. Instead
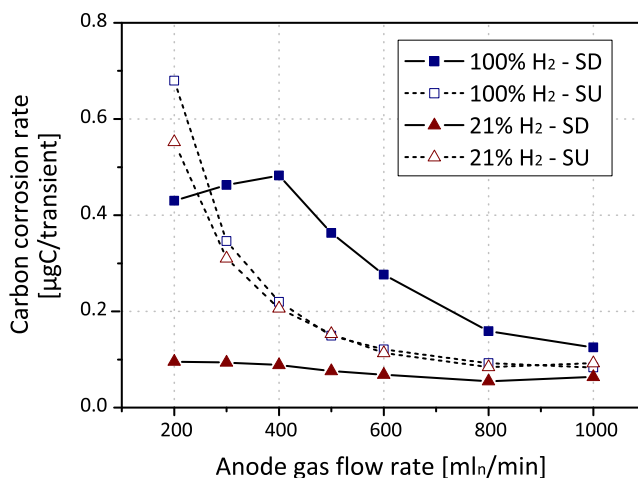

Fig. 5. Carbon corrosion rates determined for start-up (SU) and shut-down (SD) processes as a function of the anode gas flow rate for measurements carried out with different hydrogen concentrations. All measurements were carried out with air both at the positive and negative electrode while an external resistance of 3 Ωcm^2 was applied to the cell.

of a further increase in the amount of evolved CO_2, the corrosion rates become slightly smaller. Also in case of measurements carried out with a hydrogen concentration of 21%, CO_2 evolution during fuel cell shut-down differs from the behavior observed in OCV mode. Over the whole investigated gas flow range, the carbon corrosion rates only slightly increase from 0.06 to 0.09 µgC/transient. Thereby, for the highest flow rate of 1000 ml_n min^{-1}, the ratio between corrosion rates determined in response to shut-down and start-up transients is similar to the value of 0.7 obtained in OCV mode. With decreasing gas flow rate, however, this ratio continuously decreases to less than 0.2 at 200 ml_n min^{-1}, demonstrating that the applied load influences shut-down induced carbon corrosion over the entire gas flow range.

This strong decrease in shut-down induced CO_2 evolution at low gas flow rates might originate from the electrochemical consumption of hydrogen during the purging process. In case of high gas flow rates, the duration of the gas exchange process is assumed to be dominated by the propagation of the gas front through the anode compartment. Accordingly, the carbon corrosion rates increase linearly with increasing gas front residence time. If the flow rate is decreased below a critical value, however, residual hydrogen might be consumed before the propagation of the gas front through the anode compartment is completed. As a consequence, a further decrease in the gas flow rate does not further increase the duration of the coexistence of hydrogen and oxygen at the negative electrode. The time for which the positive electrode is exposed to detrimental potentials thus becomes independent of the gas flow rate. This mechanism is supported by the fact that the critical gas flow rate obviously depends on the amount of hydrogen present in the anode compartment prior to fuel cell shut-down. In case of measurements carried out with pure hydrogen, the corrosion behavior changes at flow rates lower than 400 ml_n min^{-1}. If the concentration is decreased to 21%, however, CO_2 evolution remains at a low level over the entire gas flow range, indicating that the consumption of hydrogen in the anode gas is substantially faster than in case of pure hydrogen.

Correspondingly, electrochemical hydrogen consumption also influences the gas replacement process during start-up of the fuel cell. In this case, the duration required for a complete exchange of the anode gas is expected to increase. However, owing to the continuous supply of hydrogen during fuel cell start-up, the carbon corrosion behavior is similar to that obtained in OCV mode.

In principle, the development of elevated potentials during start-up and shut-down of the fuel cell can be avoided by short circuiting the electrodes during the purging process. In case of fuel cell stacks, however, an inhomogeneous propagation of the gas front can lead to a reversal of single cells. Since the resistance can thus not be chosen arbitrarily small, start-up and shut-down of fuel cell stacks always requires a tradeoff between a homogeneous cell voltage distribution and an effective mitigation of start/stop induced catalyst support corrosion.

To quantify the mitigating effect of the applied load, carbon corrosion rates were determined as a function of the external resistance while operating the cell at a constant flow rate of 600 ml_n min^{-1} using pure hydrogen and air as reactant gases (cf. Fig. 6). Additionally, the average cell voltage during 'on' state (H_2/air mode) was determined to obtain an indication for the polarization of the electrodes in the air/air section of the fuel cell. The results show that the carbon corrosion behavior undergoes significant changes in the investigated resistance range. At low resistance values, the influence of the applied load is comparatively small. Despite an increase in the cell voltage by more than 200 mV, a change in the resistance from 0.5 to 3 Ωcm^2 increases the carbon corrosion rates for both start-up and shut-down transients only by a factor of two. This small influence of the applied load might be
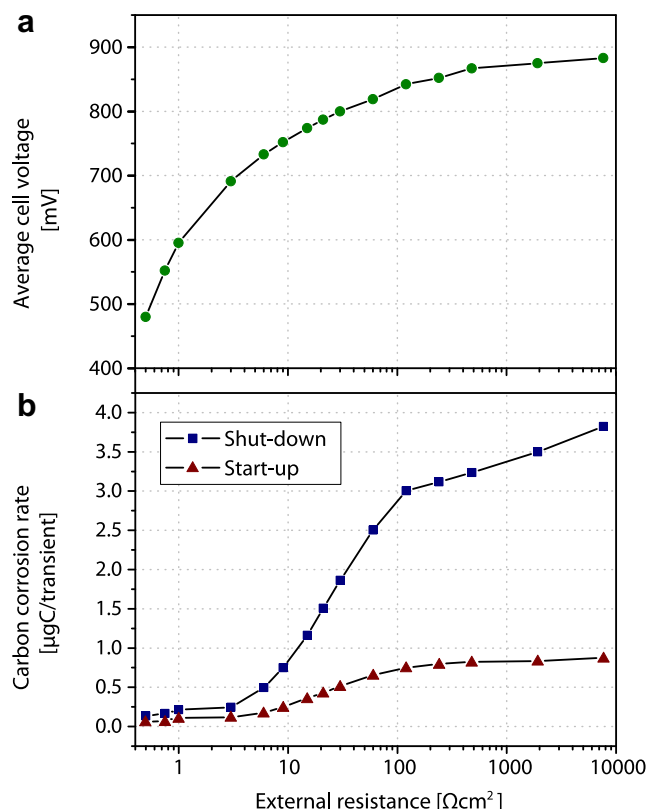

Fig. 6. (a) Influence of the external resistance on the average cell voltage during 'on' state (H_2/air mode). (b) Carbon corrosion rates determined for start-up (SU) and shut-down (SD) transients as a function of the external resistance. All measurements were carried out at a constant gas flow rate of 600 mln/min using pure hydrogen and air as reactant gases.

ascribed to a strong contribution of corrosion processes occurring in the potential range below 1 V. Due to the comparatively low voltage generated in the normal operation section of the fuel cell, the potential at the positive electrode is expected to increase only slightly above the oxygen equilibrium potential. As a consequence, a substantial fraction of the total amount of evolved CO_2 originates from the electrooxidation of CO at around 0.55 V and platinum catalyzed carbon corrosion at potentials exceeding approximately 0.7 V [6–9,33]. Thus, as long as CO_2 evolution is dominated by these processes, the effect of the applied load is comparatively small. If the external resistance is further increased, the corrosion rates become substantially higher, indicating that most of the evolved CO_2 originates from carbon corrosion at potentials exceeding 1 V. At resistance values higher than approximately 100 Ωcm^2 the effect of the applied load on both start-up and shut-down induced CO_2 evolution again becomes less pronounced. The small effect of the external load in this resistance range can be explained by the fact that a change in the resistance by almost two orders of magnitude increases the cell voltage by only 65 mV. The influence of the load on the potential developing at the positive electrode can therefore assumed to be small.

According to these processes, the external load also influences the ratios between carbon corrosion rates determined in response to shut-down and start-up transients. In the resistance range below around 3 Ωcm^2, the ratio is largely independent of the applied load. The value of around two is thereby similar to that obtained in flow variation experiments at the corresponding gas flow rate of 600 ml_n min^{-1} (cf. Fig. 5). A further increase in the external resistance results in a gradual increase in the ratio. Since the effect of the

applied load becomes less pronounced in case of high resistance values, the ratio finally approaches a largely constant value of approximately four, which is in reasonably good agreement with the ratio obtained under similar conditions in OCV mode (cf. Fig. 2).

3.3. Effect of temperature and humidity

Owing to the good control of the potential conditions at the positive electrode, the influence of decisive operating parameters on the carbon corrosion behavior is typically assessed by applying cyclic or constant potentials to cells operated in H_2/N_2 mode. Under these controlled potential conditions, the effect of temperature and reactant gas humidity has been widely studied. Since water is involved in the carbon oxidation reaction (cf. Equation (1)), the corrosion rates generally show a linear increase with increasing water vapor partial pressure [6,34]. Yet, if relative humidity is decreased below around 40%, the substantial increase in ionomer resistance can lead to significant deviations from this linear correlation [35]. In case of temperature variation, carbon corrosion behavior under controlled potential conditions typically follows an Arrhenius-dependence [6,8,10,11,27].

Catalyst support corrosion caused by real start/stop transients, however, can significantly differ from the behavior obtained under controlled potential conditions. In contrast to measurements in H_2/N_2 mode, fuel cell start-up and shut-down by purging of the anode compartment leads to a complex interaction of different processes. On the one hand, the detrimental potentials developing at the positive electrode strongly depend on the operating conditions. A change in a specific parameter thus always additionally influences the driving force for carbon corrosion. On the other hand, start/stop induced carbon corrosion behavior can be additionally affected by phenomena related to the propagation of the gas front through the anode compartment.

Fig. 7 shows the influence of temperature on the carbon corrosion rates determined in response to real start-up and shut-down processes. For temperatures up to 70 °C, the corrosion behavior follows the expected Arrhenius-dependence. Yet, the apparent activation energies of 37.5 kJ mol^{-1} (shut-down) and 33.5 kJ mol^{-1} (start-up) are considerably lower compared to the values of approximately 60 kJ mol^{-1} obtained under controlled potential conditions [6,27,36]. If the temperature is increased to values exceeding 70 °C, the corrosion behavior significantly

deviates from the Arrhenius-correlation. For both start-up and shut-down transients, the increase in CO_2 evolution becomes much less pronounced. The corresponding cell voltages determined during the 'on' state, however, vary by only about 10 mV, indicating that the driving voltage generated by the normal operation section during the purging process is not markedly influenced by the temperature. Accordingly, also the kinetics of the oxygen reduction reaction in the air/air section of the fuel cell must remain virtually unchanged. Since the potential developing at the positive electrode can therefore be assumed to be largely independent of the temperature, the observed change in carbon corrosion behavior is likely to be based on a decrease in the duration of the gas exchange process.

The accelerated propagation of the gas front might thereby be based on temperature-dependent changes in the volumetric flow of the reactant gases. Since the amount of hydrogen and air supplied to the cell is regulated via the mass of the dry gases at room temperature, the volume expansion and the addition of water vapor to the gas stream can substantially increase the effective volumetric flow. Due to the exponential correlation between temperature and water vapor partial pressure, the acceleration of the gas exchange process is thereby most pronounced in case of high temperatures. While an increase from 40 °C to 70 °C increases the gas flow rate by less than 240 ml min^{-1}, a further increase to 90 °C results in a change of the flow rate by approximately 620 ml min^{-1}. The carbon corrosion rates which would be expected without this substantial increase in the effective gas flow rate can be calculated through the activation energies determined in the temperature range below 70 °C. For a temperature of 90 °C, this estimation yields values of 0.22 and 0.49 µgC/transient for fuel cell start-up and shut-down, respectively. Considering that a doubling of the gas flow rate decreases the corrosion rates by more than a factor of two (cf. Fig. 5), the difference between the calculated and the measured values is in good agreement with the corresponding increase in the volumetric flow of the reactant gases. The deviations from the Arrhenius behavior can thus be adequately explained by the temperature-dependent changes in the effective duration of the gas exchange process. Accordingly, this phenomenon partially mitigates the detrimental effect of increased temperatures in case of real start-up and shut-down processes.

In contrast to temperature, the humidification of the reactant gases has a strong influence on the cell voltage generated in normal
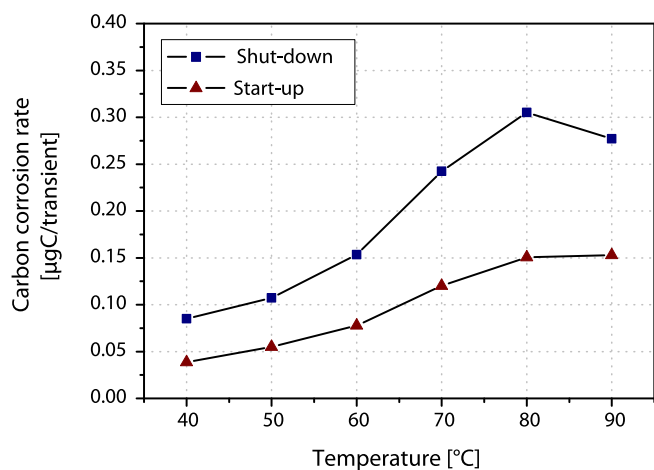

Fig. 7. Carbon corrosion rates determined in response to single start/stop transients as a function of the temperature. The measurement was carried out at a relative humidity of 70% using pure hydrogen and air as reactant gases. During start-up and shut-down, an external load of 3 Ωcm^2 was applied to the cell.
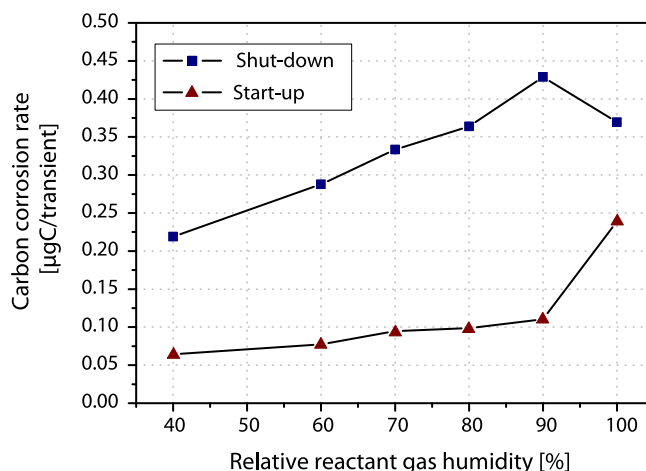

Fig. 8. Carbon corrosion rates determined in response to single start/stop transients as a function of the reactant gas humidity. The measurement was carried out at a temperature of 80 °C using pure hydrogen and air as reactant gases. During start-up and shut-down, an external load of 3 Ωcm^2 was applied to the cell.

operation mode. As a consequence of the logarithmic correlation between relative humidity and ionomer resistance in the membrane and the catalyst layer, this effect is most pronounced in case of low humidity values [35,37–39]. Between 100% and 70% R.H., the average cell voltage changes by only 15 mV while a further decrease to 40% R.H. causes an additional voltage drop of approximately 35 mV. Despite these strong changes in the cell voltage, the corrosion rates for both start-up and shut-down transients show a basically linear increase with increasing reactant gas humidity (cf. Fig. 8). This linear correlation, which is in good agreement with the behavior obtained under controlled potential conditions, suggests that the effect of reactant gas humidity on the voltage generated by the normal operation section is not sufficient to significantly influence the potential acting as driving force for carbon corrosion. Moreover, as discussed in Section 3.2, a comparatively large contribution of CO_2 evolution in the potential range below 1 V might additionally mitigate the effect of the maximum potential developing at the positive electrode.

Table 1
Summary of parameter variations and their effects on the start-up and shut-down induced carbon oxidation reaction (COR). All measurements were carried out at a cell temperature of 80 °C and a relative humidity of the gases of 70%, if not otherwise noted.

Mode	Varied parameter	Insight regarding COR
OCV[a]	Gas flow rate and concentration of H_2 and O_2 in anode compartment	• Rate of COR dominated by anode purge induced gas exchange process • Gas exchange process strongly affected by diffusion processes in the GDL and catalyst layer • Duration of reverse current situation mainly determined by the H_2 concentration (due to its high diffusivity and dominating effect on the electrode potential) • Influence of electrochemical consumption and direct recombination of H_2 and O_2, diffusion on the channel-and-land scale, and (pseudo-)capacitive currents negligible
Discharge mode[b]	Gas flow rate and H_2 concentration	• Effect on shut-down more pronounced than on start-up. • Electrochemical H_2 consumption dominates or shortens duration of reverse-current situation on shut-down. • Electrochemical H_2 consumption has little influence in the case of start-up, owing to the continuous supply of H_2.
Discharge mode	External resistance	• $R > 100 \, \Omega cm^2$: behavior similar to OCV mode • $R < 10 \, \Omega cm^2$: electrochemical H_2 consumption dominating; possibly contributions to COR from processes at electrode potentials below 1 V.
Discharge mode[b]	Cell temperature	• $T \leq 70$ °C: COR follows apparent Arrhenius behavior • $T > 70$ °C: effective gas flow rate increases with temperature due to the effects of increasing molar volume of the gas and decreasing reactant partial pressure
Discharge mode[b]	Humidity of gases	• Largely linear dependence of COR on relative humidity • At 100 % r.h. electrode flooding effects are apparent

[a] Cell temperature: 50 °C.
[b] External resistance: 3 Ωcm^2.

In case of fully humidified gases, however, the carbon corrosion behavior shows substantial deviations from the linear correlation. Corrosion rates determined for start-up processes strongly increase while fuel cell shut-down becomes less detrimental. Simultaneously, the amount of CO_2 evolving during consecutive start/stop transients becomes highly irregular, indicating an inhomogeneous propagation of the hydrogen/air front through the anode compartment. These inhomogenities might result from electrode flooding caused by the accumulation of liquid water at the negative electrode. During fuel cell start-up, the liquid water might block certain areas of the electrode, thus temporarily leading to a process similar to local fuel starvation [3,26,40–43]. The mechanisms leading to the decrease in CO_2 evolution during fuel cell shut-down, however, are largely unclear. In case of severe electrode flooding, the lower corrosion rates might possibly be attributed to a smaller area of the air/air regions during the purging process. Furthermore, changes in the carbon surface oxide composition caused by the increased corrosion intensity during start-up might contribute to the decrease in CO_2 evolution [4,5,44,45].

Yet, despite these strong deviations from the linear behavior, the overall amount of evolved CO_2 does not significantly change in case of fully humidified gases. The total carbon corrosion rate calculated by addition of the values determined for start-up and shut-down transients shows a linear correlation over the entire humidity range.

As a summary, the observed effects on varied operating parameters and proposed explanations during start-stop experiments are collated in Table 1 as an overview.

4. Conclusions

The corrosion of high surface area carbon during fuel cell start-up and shut-down by purging of the negative electrode was systematically quantified to elucidate effects related to the propagation of the gas front through the anode compartment and to determine the influence of temperature, reactant gas humidity and an applied external load.

The linear correlation between gas front residence time and carbon corrosion rate obtained in measurements with different reactant gas concentrations in OCV mode suggests that the gas exchange at the negative electrode is dominated by a uniform displacement of the anode gas. The influence of additional effects such as direct recombination of hydrogen and oxygen, diffusion on the channel and land scale and pseudocapacitive effects seem to be negligible under the investigated conditions. Generally, CO_2 evolution during fuel cell start-up is mainly controlled by the oxygen concentration while the effect of hydrogen content is more pronounced in case of fuel cell shut-down. The ratio between the corrosion rates obtained in response to start-up and shut-down transients was found to be solely determined by the hydrogen concentration.

If an external load is applied during the gas exchange process, the corrosion behavior strongly differs for fuel cell start-up and shut-down. While the linear correlation between CO_2 evolution and gas front residence time is not affected in case of start-up transients, shut-down induced carbon corrosion rates become virtually constant if the gas flow rate is decreased below a critical value. This substantial change in corrosion behavior was attributed to an acceleration of the gas exchange process by electrochemical hydrogen consumption.

Temperature and humidity variation measurements show that the corrosion behavior during start-up and shut-down by purging of the anode compartment can significantly differ from the correlations obtained under controlled potential conditions in H_2/N_2 mode. Potential cycling, which is the standard method to assess the

stability of electrode materials against elevated potentials, thus only provides limited information about start/stop durability under application relevant conditions.

Acknowledgment

References

[1] C.A. Reiser, L. Bregoli, T.W. Patterson, J.S. Yi, J.D. Yang, M.L. Perry, T.D. Jarvi, Electrochem. Solid State Lett. 8 (2005) A273–A276.
[2] H. Schulenburg, B. Schwanitz, N. Linse, G.G. Scherer, A. Wokaun, J. Krbanjevic, R. Grothausmann, I. Manke, J. Phys. Chem. C 115 (2011) 14236–14243.
[3] Z.Y. Liu, B.K. Brady, R.N. Carter, B. Litteer, M. Budinski, J.K. Hyun, D.A. Muller, J. Electrochem. Soc. 155 (2008) B979–B984.
[4] K.G. Gallagher, D.T. Wong, T.F. Fuller, J. Electrochem. Soc. 155 (2008) B488–B493.
[5] L.C. Colmenares, A. Wurth, Z. Jusys, R.J. Behm, J. Power Sources 190 (2009) 14–24.
[6] S. Maass, F. Finsterwalder, G. Frank, R. Hartmann, C. Merten, J. Power Sources 176 (2008) 444–451.
[7] W. Li, A.M. Lane, Electrochem. Commun. 11 (2009) 1187–1190.
[8] L.M. Roen, C.H. Paik, T.D. Jarvi, Electrochem. Solid State Lett. 7 (2004) A19–A22.
[9] J. Willsau, J. Heitbaum, J. Electroanal. Chem. 161 (1984) 93–101.
[10] S.C. Ball, S.L. Hudson, D. Thompsett, B. Theobald, J. Power Sources 171 (2007) 18–25.
[11] B.R. Wickman, H. Grönbeck, P. Hanarp, B. Kasemo, J. Electrochem. Soc. 157 (2010) B592–B598.
[12] K.H. Lim, H.-S. Oh, S.-E. Jang, Y.-J. Ko, H.-J. Kim, H. Kim, J. Power Sources 193 (2009) 575–579.
[13] A. Chaparro, N. Mueller, C. Atienza, L. Daza, J. Electroanal. Chem. 591 (2006) 69–73.
[14] H.-S. Oh, K.H. Lim, B. Roh, I. Hwang, H. Kim, Electrochim. Acta 54 (2009) 6515–6521.
[15] K. Mayrhofer, J. Meier, S. Ashton, G. Wiberg, F. Kraus, M. Hanzlik, M. Arenz, Electrochem. Commun. 10 (2008) 1144–1147.
[16] R. Borup, J. Davey, F. Garzon, D. Wood, M. Inbody, J. Power Sources 163 (2006) 76–81.
[17] W. Bi, T.F. Fuller, J. Electrochem. Soc. 155 (2008) B215–B221.
[18] G. Maranzana, O. Lottin, T. Colinart, S. Chupin, S. Didierjean, J. Power Sources 180 (2008) 748–754.
[19] Z. Siroma, N. Fujiwara, T. Ioroi, S. Yamazaki, H. Senoh, K. Yasuda, K. Tanimoto, J. Power Sources 172 (2007) 155–162.
[20] G. Maranzana, C. Moyne, J. Dillet, S. Didierjean, O. Lottin, J. Power Sources 195 (2010) 5990–5995.
[21] H. Fukumoto, S. Yoshioka, S. Matsumoto. PEM Fuel Cells 8, ECS Trans. 16 (2) (2008) 841–847.
[22] I.A. Schneider, S. von Dahlen, Electrochem. Solid State Lett. 14 (2011) B30–B33.
[23] K.G. Gallagher, G. Yushin, T.F. Fuller, J. Electrochem. Soc. 157 (2010) B820–B830.
[24] S.J. Ashton, M. Arenz, Electrochem. Commun. 13 (2011) 1473–1475.
[25] J. Kim, J. Lee, Y. Tak, J. Power Sources 192 (2009) 674–678.
[26] W.R. Baumgartner, P. Parz, S.D. Fraser, E. Wallnöfer, V. Hacker, J. Power Sources 182 (2008) 413–421.
[27] N. Takeuchi, T.F. Fuller, J. Electrochem. Soc. 157 (2010) B135–B140.
[28] J.H. Kim, E.A. Cho, J.H. Jang, H.J. Kim, T.H. Lim, I.H. Oh, J.J. Ko, I.-J. Son, J. Electrochem. Soc. 157 (2010) B118–B124.
[29] H. Chizawa, Y. Ogami, H. Naka, A. Matsunaga, N. Aoki, T. Aoki, K. Tanaka. PEM Fuel Cells 7, ECS Trans. 11 (1) (2007) 981–992.
[30] Y. Ishigami, K. Takada, H. Yano, J. Inukai, M. Uchida, Y. Nagumo, T. Hyakutake, H. Nishide, M. Watanabe, J. Power Sources 196 (2011) 3003–3008.
[31] W. Gu, R.N. Carter, P.T. Yu, H.A. Gasteiger. PEM Fuel Cells 7, ECS Trans. 11 (1) (2007) 963–973.
[32] I.V. Ivchenko, S.K. Loyalka, R.V. Tompson, Analytical Methods for Problems of Molecular Transport, Springer, 2010.
[33] N. Linse, L. Gubler, G.G. Scherer, A. Wokaun, Electrochim. Acta 56 (2011) 7541–7549.
[34] N. Linse, C. Aellig, A. Wokaun, G.G. Scherer, L. Gubler. PEM Fuel Cells 9, ECS Trans. 25 (1) (2009) 1849–1859.
[35] N. Linse, G.G. Scherer, A. Wokaun, L. Gubler, Electrochemistry Laboratory - Annual Report 2010, ISSN 1661-5379 (2011), Can be downloaded from, http://ecl.web.psi.ch/SciRep.html. pp. 82–83.
[36] N. Linse, PhD Thesis, ETH Zurich, Diss. ETH No. 20132, 2012 (http://dx.doi.org/10.3929/ethz-a-007110293).
[37] S. Ochi, O. Kamishima, J. Mizusaki, J. Kawamura, Solid State Ionics 180 (2009) 580–584.
[38] H. Iden, A. Ohma, K. Shinohara, J. Electrochem. Soc. 156 (2009) B1078–B1084.
[39] C.K. Mittelsteadt, H. Liu, in: W. Vielstich, H. Yokokawa, H.A. Gasteiger (Eds.), Handbook of Fuel Cells Volume 5-Advances in Electrocatalysis, Materials, Diagnostics and Durability, John Wiley & Sons, 2009, pp. 345–357.
[40] T.W. Patterson, R.M. Darling, Electrochem. Solid State Lett. 9 (2006) A183–A185.
[41] Z. Liu, L. Yang, Z. Mao, W. Zhuge, Y. Zhang, L. Wang, J. Power Sources 157 (2006) 166–176.
[42] A. Taniguchi, T. Akita, K. Yasuda, Y. Miyazaki, J. Power Sources 130 (2004) 42–49.
[43] D. Liang, Q. Shen, M. Hou, Z. Shao, B. Yi, J. Power Sources 194 (2009) 847–853.
[44] K.G. Gallagher, T.F. Fuller, Phys. Chem.y Chem. Phys. 11 (2009) 11557–11567.
[45] Y. Shao, J. Wang, R. Kou, M. Engelhard, J. Liu, Y. Wang, Y. Lin, Electrochim. Acta 54 (2009) 3109–3114.